Designed nonlocal pseudopotentials for enhanced transferability

Nicholas J. Ramer and Andrew M. Rappe
Department of Chemistry and Laboratory for Research on the Structure of Matter, University of Pennsylvania, Philadelphia, Pennsylvania 19104
(Received 4 November 1998)

A pseudopotential generation method is presented which significantly improves transferability. The method exploits flexibility contained in the separable Kleinman-Bylander form of the nonlocal pseudopotential [Phys. Rev. Lett. **48**, 1425 (1982)]. By adjusting the functional form of the local potential, we are able to improve the agreement with all-electron calculations. Results are presented for the H, Si, Ca, Zr, and Pb atomic pseudopotentials. Configuration testing, logarithmic derivatives, chemical hardness, and structural tests all confirm the accuracy of these pseudopotentials. [S0163-1829(99)14715-5]

I. INTRODUCTION

The pseudopotential approximation, or the separation of electrons into core and valence based on their level of participation in chemical bonding, is central to most modern electronic structure calculations. The original atomic pseudopotential formalism[1] grew out of the orthogonalized plane-wave approach.[2] The pseudopotential replaces the nuclear Coulomb potential plus core electrons, thus simplifying the original system of differential equations. Adopting the pseudopotential approximation may introduce some unphysical results if the pseudopotentials are not constructed judiciously. The accuracy of the pseudopotential, or its transferability, may be gauged by its ability to reproduce the results of all-electron calculations in a variety of atomic environments.

The earliest pseudopotentials generated for use in density-functional theory calculations replaced the strongly attractive Coulombic potential near the origin with a weaker local potential, and core electrons were eliminated from the calculations.[3] In this approach, approximate agreement between pseudopotential and all-electron eigenvalues as well as logarithmic derivatives was achieved for many elements. However, first-row nonmetals and first-row transition metals could not be accurately described by these pseudopotentials.

To improve pseudopotential transferability, more complicated (and more flexible) semilocal pseudopotentials were designed[4] with a different spherically symmetric potential for each angular momentum. This added flexibility permits the enforcement of the norm-conservation condition at the reference energy, ε_i, for R greater than the core radius, r_c

$$\frac{d}{d\varepsilon}\left(\frac{d\ln\phi_i^{\mathrm{AE}}(\mathbf{r})}{dr}\right)\bigg|_{R,\varepsilon_i}=\frac{d}{d\varepsilon}\left(\frac{d\ln\phi_i^{\mathrm{PS}}(\mathbf{r})}{dr}\right)\bigg|_{R,\varepsilon_i}, \qquad (1)$$

where $\phi_i^{\mathrm{AE}}(\mathbf{r})$ and $\phi_i^{\mathrm{PS}}(\mathbf{r})$ are the all-electron and pseudopotential Kohn-Sham eigenstates for the state i. Including this criterion into pseudopotential generation greatly improves transferability.

Incorporating norm conservation makes it possible to have exact agreement between the all-electron and pseudopotential eigenvalues and wave functions outside r_c for one electronic reference state.[4] However, the corresponding single-particle differential equation for a pseudopotential constructed with this method is more complicated because of the angular momentum projection. Expressing the semilocal pseudopotentials within a plane-wave basis requires the computation of $V(\mathbf{G},\mathbf{G}')$ instead of just $V(\mathbf{G}-\mathbf{G}')$, where $\mathbf{G}$ is a reciprocal-lattice vector. This results in a huge memory expense.

The fully separable nonlocal Kleinman-Bylander pseudopotential form[5] dramatically reduces the memory cost of the semilocal pseudopotentials. These pseudopotentials are constructed from a local potential and angular-momentum-dependent nonlocal projectors. In Fourier space, the projector can be expressed as $W(\mathbf{G})\cdot W(\mathbf{G}')$ replacing $V(\mathbf{G},\mathbf{G}')$. This reduces the pseudopotential memory scaling from N^2 to N. With the inclusion of the nonlocal projectors, the resulting single-particle Kohn-Sham equation becomes an integrodifferential equation. The solutions to an integrodifferential equation may violate the Wronskian theorem and possess noded eigenstates lower in energy than the nodeless solution.[6] A simple diagnostic procedure[7] allows for detection of these lower-energy or ghost states. The separable form of these potentials also permits efficient evaluation in solid-state calculations with N^2 or $N^2\log_2 N$ CPU time scaling[8,9] for the nonlocal energy contribution and its gradients. These potentials have proven very effective for the study of computationally intensive large-scale systems.[10]

To improve the transferability of the Kleinman-Bylander pseudopotentials, multiple-projector separable nonlocal pseudopotentials have been developed.[11,12] In these approaches, the Kleinman-Bylander nonlocal projector form is considered the first term of a series expansion of projectors. These projectors provide agreement of the pseudoatom scattering properties over a broader energy range.

While characterization of the scattering properties is an important tool in ascertaining the transferability of a pseudopotential, there are some properties that cannot be sampled using this diagnostic. These remaining properties involve effects of electrostatic screening and nonlinearity of the exchange-correlation energy. Recently, chemical hardness conservation has been used as an effective measure of how these self-consistent terms vary with electronic configuration

and as an indication of accurate pseudopotential generation.[13] The chemical hardness is defined as the matrix

$$H_{nl,n'l'}=\frac{1}{2}\frac{\partial^2 E_{\rm tot}[\rho(\mathbf{r})]}{\partial f_{nl}\partial f_{n'l'}}=\frac{1}{2}\frac{\partial \varepsilon_{nl}}{\partial f_{n'l'}}, \tag{2}$$

where $E_{\rm tot}[\rho(\mathbf{r})]$ is the total energy of the atom and is a functional of the total electronic charge density $\rho(\mathbf{r})$, f_{nl} is the occupation number of the nlth state, and ε_{nl} is the self-consistent nlth eigenvalue. In the second equality, we have used the fact that $\varepsilon_{nl}=\partial E_{\rm tot}[\rho(\mathbf{r})]/\partial f_{nl}$.

One of the other major objectives in pseudopotential generation, besides transferability, is rapid convergence in a plane-wave basis. It has been shown that the residual kinetic energy of the reference state pseudo-wave-functions lying beyond the plane-wave cutoff energy is an excellent predictor of the basis set convergence error of the pseudopotential in a solid or molecule.[14] The optimized pseudopotential construction is designed to minimize this residual kinetic energy.

The ultrasoft pseudopotential construction[12] was formulated to generate highly transferable multiple-projector pseudopotentials with rapid convergence in a plane-wave basis. In order to improve pseudo-wave-function smoothness, the norm-conservation constraint on the wave function is relaxed. To reintroduce norm conservation, a compensating valence charge density is added.

In this paper, we present a method for nonlocal pseudopotential construction according to the Kleinman-Bylander separable form which improves accuracy while retaining the convenience of a single-projector representation. We exploit the inherent arbitrariness in the separation of the local and nonlocal components of the potential. The present work should be placed in context with other recent studies that have focused on this same flexibility. One such study involved constructing the local potentials from various linear combinations of the semilocal potentials.[15] Chemical hardness testing showed that the accuracy of these pseudopotentials approached the accuracy of a semilocal pseudopotential from the same set of l-dependent potentials, but did not exceed it. In another study, the form of the local potential is expressed as a sum of Gaussians for the first two rows of the Periodic Table.[16] These dual-space multiple-projector pseudopotentials have more recently been extended to include the scalar relativistic effect.[17] Using this approach, a high level of transferability can be obtained for elements up to Rn.

The paper is organized as follows. We give a brief review of the Kleinman-Bylander nonlocal pseudopotential formalism in Sec. II. We also illustrate our approach for improving transferability. In Sec. III, we present atomic and solid-state testing results for potentials constructed with our form of the nonlocal components for the H, Si, Ca, Zr, and Pb atoms. Conclusions are presented in Sec. IV.

II. DESIGNED NONLOCAL PSEUDOPOTENTIAL FORMALISM

To construct a pseudopotential, an electronic reference state is chosen, and an all-electron calculation is performed. From this calculation we obtain the all-electron potential ($\hat{V}_{\rm AE}$), the total energy ($E_{\rm tot}^{\rm AE}$), the all-electron wave functions ($\phi_{nl}^{\rm AE}(\mathbf{r})$) and their eigenvalues ($\varepsilon_{nl}^{\rm AE}$). Then a pseudopotential $\hat{V}_{\rm PS}$ and pseudo-wave-functions $|\phi_{nl}^{\rm PS}\rangle$ are chosen which satisfy

$$(\hat{T}+\hat{V}_{\rm H}[\rho]+\hat{V}_{\rm XC}[\rho]+\hat{V}_{\rm PS})|\phi_{nl}^{\rm PS}\rangle=\varepsilon_{nl}|\phi_{nl}^{\rm PS}\rangle, \tag{3}$$

where $\hat{T}$ is the single-particle kinetic-energy operator, and $\hat{V}_{\rm H}[\rho]$ and $\hat{V}_{\rm XC}[\rho]$ are the self-consistent Hartree and exchange-correlation energy operators, respectively. The latter two operators are functionals of the total charge density $\rho(\mathbf{r})$, where $\rho(\mathbf{r})=\Sigma_{nl}f_{nl}|\phi_{nl}^{\rm PS}(\mathbf{r})|^2$. We require that the pseudo-wave-functions obey the following criteria:

(1) $\phi_{nl}^{\rm PS}(\mathbf{r})=\phi_{nl}^{\rm AE}(\mathbf{r})$, $\dfrac{d\phi_{nl}^{\rm PS}(\mathbf{r})}{dr}=\dfrac{d\phi_{nl}^{\rm AE}(\mathbf{r})}{dr}$, $\dfrac{d^2\phi_{nl}^{\rm PS}(\mathbf{r})}{dr^2}=\dfrac{d^2\phi_{nl}^{\rm AE}(\mathbf{r})}{dr^2}$ for $r\geq r_c$.

(2) $\varepsilon_{nl}^{\rm PS}=\varepsilon_{nl}^{\rm AE}$.

(3) $$\frac{d}{d\varepsilon}\left(\frac{d\ln\phi_{nl}^{\rm PS}(\mathbf{r})}{dr}\right)\bigg|_{R,\varepsilon_{nl}}=\frac{d}{d\varepsilon}\left(\frac{d\ln\phi_{nl}^{\rm AE}(\mathbf{r})}{dr}\right)\bigg|_{R,\varepsilon_{nl}}$$

.

(4) $\langle\phi_{nl}^{\rm PS}|\phi_{nl}^{\rm PS}\rangle=\langle\phi_{nl}^{\rm AE}|\phi_{nl}^{\rm AE}\rangle=1$.

If $\hat{V}_{\rm PS}$ is not l dependent, the resulting pseudopotential is called local (radially and angularly local). More generally, $\hat{V}_{\rm PS}$ can be separated into a local potential and a sum of short-ranged corrections:

$$\hat{V}_{\rm PS}=\hat{V}^{\rm loc}+\sum_l \Delta\hat{V}_l, \tag{4}$$

where

$$\hat{V}^{\rm loc}\equiv\int d^3r|\mathbf{r}\rangle V^{\rm loc}(\mathbf{r})\langle\mathbf{r}|. \tag{5}$$

For a semilocal pseudopotential, the corrections $\Delta\hat{V}_l^{\rm SL}$ are projection operators in the angular coordinates and local in the radial coordinate. To construct a fully separable nonlocal pseudopotential, $\Delta\hat{V}_l$ is formed according to

$$\Delta\hat{V}_l^{\rm NL}\equiv\frac{\Delta\hat{V}_l^{\rm SL}|\phi_{nl}^{\rm PS}\rangle\langle\phi_{nl}^{\rm PS}|\Delta\hat{V}_l^{\rm SL}}{\langle\phi_{nl}^{\rm PS}|\Delta\hat{V}_l^{\rm SL}|\phi_{nl}^{\rm PS}\rangle}. \tag{6}$$

When $\hat{V}_{\rm PS}$ operates on $|\phi_{nl}^{\rm PS}\rangle$, we obtain

$$\hat{V}_{\rm PS}|\phi_{nl}^{\rm PS}\rangle=(\hat{V}^{\rm loc}+\Delta\hat{V}_l^{\rm SL})|\phi_{nl}^{\rm PS}\rangle. \tag{7}$$

Therefore, for the reference configuration we are guaranteed exact agreement between the eigenvalues and wave functions of the semilocal and nonlocal atoms.

However, for any state $|\psi_{n'l}^{\rm PS}\rangle$ other than the reference state,

$$\hat{V}_{\rm PS}|\psi_{n'l}^{\rm PS}\rangle\neq(\hat{V}^{\rm loc}+\Delta\hat{V}_l^{\rm SL})|\psi_{n'l}^{\rm PS}\rangle, \tag{8}$$

where n' is not required to equal n. The inequality in Eq. (8) illustrates the difficulties involved in assessing and improving the transferability of nonlocal pseudopotentials: the

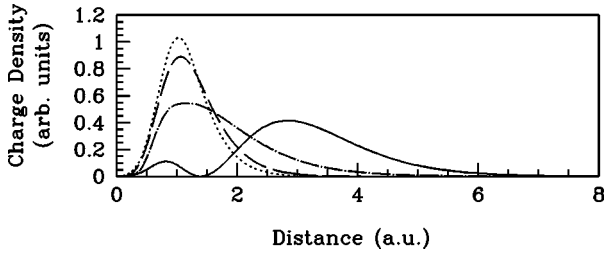

FIG. 1. Radial charge-density distribution for the Ca^{+2} pseudo-atom ($3s^2 3p^6 4s^0 3d^0$). Results are given for $3s$ (dotted line), $3p$ (dashed line), $4s$ (solid line), and $3d$ states (dot-dashed line).

transferability of a nonlocal pseudopotential can be dramatically different from the corresponding semilocal pseudopotential.

For simplicity, we have focused on the single-projector nonlocal pseudopotential construction in the current approach. We begin by constructing an optimized semilocal pseudopotential. Since Eq. (4) is simply an addition of local and nonlocal terms, we may alter $\hat{V}^{\rm loc}$ arbitrarily without losing the exact agreement between the all-electron and nonlocal eigenvalues and pseudo-wave-functions at the reference state, *provided* we adjust the nonlocal corrections accordingly. However, we change the eigenvalue agreement at any other configuration by doing so.

Operationally, additional electronic configurations or design configurations are chosen. A local augmentation operator ($\hat{A}$) is added to the local potential forming a designed nonlocal pseudopotential. The augmentation operator is subtracted from the nonlocal corrections $\Delta\hat{V}_l$ in the following way:

$$\hat{V}_{\rm PS}=(\hat{V}^{\rm loc}+\hat{A})+\sum_l \Delta\hat{V}_l^{\rm DNL}, \tag{9}$$

TABLE I. Construction parameters for the H, Si, Ca, Zr, and Pb pseudopotentials. HSC potentials were generated with the method described in Ref. 4. OPT potentials were generated with methods described in Ref. 14. Core radii (r_c) are in atomic units, q_c are in $Ry^{1/2}$, and plane-wave cutoffs ($E_{\rm cut}$) are in Ry.

Atom	Reference configuration	HSC		OPT		
		r_c	$E_{\rm cut}$	r_c	q_c	$E_{\rm cut}$
H	$1s^{0.5}$	0.35	70	0.72	7.07	50
Si	$3s^2$	1.21	16	1.90	3.60	13
	$3p^{0.5}$	1.18		1.90	3.60	
	$3d^{0.5}$	1.31		2.20	3.60	
Ca	$3s^2$	0.74	83	1.29	7.07	50
	$3p^6$	1.15		1.60	7.07	
	$3d^0$	0.70		1.27	7.07	
Zr	$4s^2$	0.92	92	1.80	7.07	50
	$4p^6$	0.81		1.51	7.07	
	$4d^0$	1.15		1.90	7.07	
Pb	$6s^0$	1.10	72	1.70	6.05	50
	$6p^0$	1.20		2.00	5.52	
	$5d^{10}$	1.10		1.75	7.07	

TABLE II. Parameters for the augmentation operator ($\hat{A}$) for the designed nonlocal pseudopotentials. Step widths are in atomic units, and step heights are in Ry.

Atom	Step width	Step height
H	0.70	2.00
Si	1.35	70.00
Ca	0.93	6.76
Zr	1.72	0.66
Pb	1.90	1.60

where

$$\Delta\hat{V}_l^{\rm DNL}=\frac{(\Delta\hat{V}_l^{\rm SL}-\hat{A})|\phi_{nl}^{\rm PS}\rangle\langle\phi_{nl}^{\rm PS}|(\Delta\hat{V}_l^{\rm SL}-\hat{A})}{\langle\phi_{nl}^{\rm PS}|(\Delta\hat{V}_l^{\rm SL}-\hat{A})|\phi_{nl}^{\rm PS}\rangle}. \tag{10}$$

When the augmented $\hat{V}_{\rm PS}$ operates on the reference state, the result reduces to Eq. (7). In doing so we are not only guaranteed the exact agreement of the nonlocal pseudopotential eigenvalues with the semilocal eigenvalues due to the Kleinman-Bylander construction but we also insure agreement with the all-electron eigenvalues due to the semilocal construction. However for any state other than the reference state, the second term in Eq. (9) will contribute differently.

By adjusting $\hat{A}$, it is possible to obtain almost exact agreement between the all-electron and designed nonlocal eigenvalues for the manifold of design configurations. With the proper selection of the reference electronic configuration and pseudopotential construction parameters, excellent transferability can be obtained for a variety of ionized and excited configurations.

The position of $\hat{A}$ deserves particular attention. We begin by examining the transferability error of a standard Kleinman-Bylander nonlocal pseudopotential constructed in the absence of an augmentation operator. Based on these results we can determine optimal placement of $\hat{A}$ in the radial grid. We have identified two different cases for the positioning of the operator.

(1) The valence orbitals may have different charge-density profiles which lead to spatial separation among the states. This situation allows placement of the augmentation operator in a region that will preferentially affect certain states while leaving other states nearly unchanged.

(2) Due to electrostatics, as an atom becomes more positively charged its charge density will move inward toward the nucleus of the atom. Positioning of the operator can therefore be made according to desired adjustments of various ionized configurations.

As an example, we have found that for the Ca nonlocal pseudopotential, the magnitudes of the transferability errors of the $3s$, $3p$, and $3d$ orbitals increase as the pseudo-atom becomes less ionized (see Table III). However, the magnitude of the error in the $4s$ orbital decreases over this same range of ionization. Therefore, the augmentation is required to adjust the $n=3$ orbitals preferentially. Figure 1 shows the charge density distribution of the Ca pseudo-atom in the $+2$ configuration. We find that there is a spatial separation be-

TABLE III. Configuration testing for the H, Si, and Ca atoms. Eigenvalues and ΔE_{tot} are given for an all-electron atom (AE). Absolute errors are given for a nonlocal pseudopotential generated with the method described in Ref. 4 (HSC), an optimized nonlocal pseudopotential generated with the method described in Ref. 14 (OPT), and a designed nonlocal pseudopotential generated with the presented method (DNL). The design configurations used to construct the DNL potentials are identified with a dagger (†). All energies are in Ry.

State	AE energy	HSC error	OPT error	DNL error	State	AE energy	HSC error	OPT error	DNL error
				H					
$1s^0$	−1.0000	0.0000	−0.0001	−0.0001	$1s^1$	−0.4673	0.0000	0.0000	0.0000
$^{\dagger}\Delta E_{\text{tot}}$	0.5504	0.0000	0.0000	0.0000	$^{\dagger}\Delta E_{\text{tot}}$	−0.3413	0.0000	0.0000	0.0000
$1s^{0.5}$	−0.9067	0.0000	0.0000	0.0000	$1s^{1.5}$	−0.1133	0.0000	0.0000	0.0000
ΔE_{tot}	0.0000	0.0000	0.0000	0.0000	$^{\dagger}\Delta E_{\text{tot}}$	−0.4819	0.0000	0.0000	0.0000
				Si					
$3s^2$	−1.4870	0.0000	0.0000	0.0000	$3s^2$	−1.4007	−0.0012	−0.0010	−0.0007
$3p^{0.5}$	−0.9406	0.0000	0.0000	0.0000	$3p^1$	−0.8647	−0.0009	−0.0008	−0.0006
$3d^{0.5}$	−0.3270	0.0000	0.0000	0.0000	$3d^0$	−0.2689	0.0001	0.0000	0.0000
ΔE_{tot}	0.0000	0.0000	0.0000	0.0000	$^{\dagger}\Delta E_{\text{tot}}$	−0.3015	−0.0002	−0.0002	−0.0001
$3s^1$	−2.1516	0.0051	0.0050	0.0040	$3s^2$	−1.2890	0.0000	0.0000	0.0000
$3p^1$	−1.5641	0.0038	0.0040	0.0032	$3p^{0.5}$	−0.7492	0.0000	0.0000	0.0000
$3d^0$	−0.8310	0.0019	0.0030	0.0025	$3d^{1.0}$	−0.1756	0.0000	0.0000	0.0000
$^{\dagger}\Delta E_{\text{tot}}$	1.4690	−0.0015	−0.0016	−0.0012	$^{\dagger}\Delta E_{\text{tot}}$	−0.1240	0.0000	0.0000	0.0000
$3s^2$	−0.7966	−0.0017	−0.0018	−0.0008	$3s^1$	−0.8514	−0.0010	−0.0011	−0.0005
$3p^2$	−0.3071	−0.0009	−0.0011	−0.0005	$3p^3$	−0.3491	−0.0007	−0.0008	−0.0003
$^{\dagger}\Delta E_{\text{tot}}$	−0.8778	−0.0013	−0.0013	−0.0001	$^{\dagger}\Delta E_{\text{tot}}$	−0.3817	−0.0007	−0.0008	−0.0005
				Ca					
$3s^2$	−4.5277	0.0000	0.0000	0.0000	$3s^2$	−3.2284	0.0039	0.0021	0.0005
$3p^6$	−3.1688	0.0000	0.0000	0.0000	$3p^6$	−1.8875	0.0007	0.0023	0.0007
$4s^0$	−1.0537	−0.0087	−0.0099	0.0000	$4s^1$	−0.2469	−0.0022	−0.0022	0.0001
$3d^0$	−1.1933	0.0000	0.0000	0.0000	$3d^1$	−0.0648	0.0012	0.0012	0.0000
$^{\dagger}\Delta E_{\text{tot}}$	0.0000	0.0000	0.0000	0.0000	ΔE_{tot}	−1.1903	−0.0119	−0.0036	−0.0001
$3s^2$	−3.9220	0.0061	0.0059	0.0000	$3s^2$	−4.4495	0.0189	0.0199	0.0003
$3p^6$	−2.5681	0.0050	0.0057	0.0000	$3p^5$	−3.0670	0.0258	0.0192	0.0007
$4s^1$	−0.6716	−0.0033	−0.0039	0.0000	$4s^2$	−0.8070	−0.0040	−0.0045	0.0000
$3d^0$	−0.6401	0.0043	0.0044	0.0000	$3d^0$	−1.0294	0.0142	0.0156	0.0006
ΔE_{tot}	−0.8746	−0.0079	−0.0062	0.0000	ΔE_{tot}	1.2031	−0.0097	−0.0223	−0.0003
$3s^2$	−3.4115	0.0095	0.0093	0.0000	$3s^2$	−5.0789	0.0129	0.0139	0.0004
$3p^6$	−2.0601	0.0078	0.0089	0.0000	$3p^5$	−3.6924	0.0212	0.0135	0.0009
$4s^2$	−0.2833	−0.0010	−0.0011	0.0000	$4s^1$	−1.2845	−0.0085	−0.0095	0.0001
$3d^0$	−0.1659	0.0061	0.0064	0.0000	$3d^0$	−1.6335	0.0098	0.0111	0.0009
$^{\dagger}\Delta E_{\text{tot}}$	−1.3478	−0.0112	−0.0086	0.0000	ΔE_{tot}	2.2464	−0.0014	−0.0155	−0.0003

tween the $n=3$ and $4s$ charge densities. In order to maximize the effectiveness of $\hat{A}$, it should be positioned between $r=0$ and $r=1$ a.u.

III. RESULTS AND DISCUSSION

We have applied the designed nonlocal pseudopotential approach to the H, Si, Ca, Zr, and Pb atoms. All atomic energy calculations were done within the local-density approximation (LDA) and optimized pseudopotential generation methods were used. For the Zr and Pb atoms, we have included the scalar relativistic effect.[18] The parameters used in the pseudopotential construction are presented in Table I. We have chosen the s angular momentum channel to be the foundation for the local potential, and a square step in the radial coordinate as our augmentation operator. (These choices are made for simplicity. Choosing other angular momentum channels for the local potential or using a multiple-step augmentation operator can lead to enhanced transferability or efficiency.) The height and width of the step have been adjusted to reproduce the all-electron eigenvalues for the design configuration.

Our selection of reference configurations deserves additional mention. Semicore orbitals were included as valence in the Ca ($3s$ and $3p$), Zr ($4s$ and $4p$), and Pb ($5d$) pseudopotentials. The inclusion of these states allowed for the removal of ghost levels, greater local potential design flexibility, and better overall transferability of the pseudopotential.

TABLE IV. Configuration testing for the Zr and Pb atoms. Eigenvalues and $\Delta E_{\rm tot}$ are given for an all-electron atom (AE). Absolute errors are given for a nonlocal pseudopotential generated with the method described in Ref. 4 (HSC), an optimized nonlocal pseudopotential generated with the method described in Ref. 14 (OPT) and a designed nonlocal pseudopotential generated with the presented method (DNL). The design configurations used to construct the DNL potentials are identified with a dagger (†). All energies are in Ry.

State	AE energy	HSC error	OPT error	DNL error	State	AE energy	HSC error	OPT error	DNL error
				Zr					
$4s^2$	−7.0190	0.0000	0.0000	0.0000	$4s^2$	−3.7412	−0.0077	−0.0079	−0.0011
$4p^6$	−5.3582	0.0000	0.0000	0.0000	$4p^6$	−2.1484	−0.0043	−0.0048	0.0000
$5s^0$	−2.4422	−0.0553	−0.0552	−0.0007	$5s^0$	−0.2693	−0.0083	−0.0088	0.0010
$4d^0$	−2.9835	0.0000	0.0000	0.0000	$4d^4$	−0.1251	−0.0001	−0.0004	0.0007
$^{\dagger}\Delta E_{\rm tot}$	0.0000	0.0000	0.0000	0.0000	$\Delta E_{\rm tot}$	−5.4996	−0.0123	−0.0106	0.0019
$4s^2$	−5.3220	0.0104	0.0106	0.0008	$4s^2$	−5.4808	0.0089	0.0111	−0.0017
$4p^6$	−3.6964	0.0102	0.0104	0.0007	$4p^5$	−3.8375	0.0105	0.0118	−0.0004
$5s^1$	−1.3047	−0.0211	−0.0215	0.0019	$5s^1$	−1.3385	−0.0252	−0.0253	0.0011
$4d^1$	−1.4711	0.0075	0.0082	0.0000	$4d^2$	−1.5623	0.0101	0.0108	0.0010
$\Delta E_{\rm tot}$	−4.0782	−0.0309	−0.0303	0.0013	$\Delta E_{\rm tot}$	−1.8274	−0.0325	−0.0320	0.0016
$4s^2$	−3.9956	0.0119	0.0118	0.0000	$4s^2$	−3.8446	−0.0003	−0.0005	−0.0005
$4p^6$	−2.3881	0.0125	0.0124	0.0002	$4p^6$	−2.2458	0.0019	0.0015	0.0002
$5s^2$	−0.3371	−0.0062	−0.0065	0.0011	$5s^1$	−0.2957	−0.0075	−0.0079	0.0012
$4d^2$	−0.2760	0.0097	0.0100	0.0000	$4d^3$	−0.1835	0.0032	0.0032	0.0006
$^{\dagger}\Delta E_{\rm tot}$	−5.7174	−0.0348	−0.0340	0.0030	$\Delta E_{\rm tot}$	−5.6291	−0.0217	−0.0203	0.0023
				Pb					
$6s^0$	−3.5516	0.0000	0.0000	0.0000	$6s^0$	−2.8615	−0.0014	−0.0019	−0.0013
$6p^0$	−2.6398	0.0000	0.0000	0.0000	$6p^1$	−2.0243	−0.0002	−0.0007	−0.0006
$5d^{10}$	−4.5497	0.0000	0.0000	0.0000	$5d^{10}$	−3.7642	−0.0048	−0.0060	−0.0045
$\Delta E_{\rm tot}$	0.0000	0.0000	0.0000	0.0000	$^{\dagger}\Delta E_{\rm tot}$	−2.3331	−0.0007	−0.0005	−0.0004
$6s^1$	−2.1243	−0.0022	−0.0031	−0.0016	$6s^1$	−1.5149	−0.0017	−0.0025	−0.0010
$6p^1$	−1.3651	−0.0007	−0.0013	−0.0011	$6p^2$	−0.8161	0.0009	0.0003	0.0003
$5d^{10}$	−2.9194	−0.0044	−0.0056	−0.0010	$5d^{10}$	−2.2559	−0.0068	−0.0084	−0.0036
$^{\dagger}\Delta E_{\rm tot}$	−4.8228	−0.0031	−0.0031	−0.0019	$^{\dagger}\Delta E_{\rm tot}$	−5.9090	−0.0033	−0.0037	−0.0024
$6s^2$	−0.8961	−0.0002	−0.0010	−0.0009	$6s^2$	−1.4323	−0.0024	−0.0034	−0.0013
$6p^2$	−0.2777	0.0030	0.0027	0.0026	$6p^1$	−0.7556	−0.0001	−0.0008	−0.0006
$5d^{10}$	−1.5607	−0.0039	−0.0054	0.0015	$5d^{10}$	−2.1339	−0.0039	−0.0053	0.0018
$^{\dagger}\Delta E_{\rm tot}$	−7.1077	−0.0049	−0.0057	−0.0027	$^{\dagger}\Delta E_{\rm tot}$	−6.5967	−0.0061	−0.0064	−0.0035

It is also important to note that although we have included multiple *s*-channel states, we do *not* treat these states with different projection operators. The pseudopotentials are generated using only one nonlocal projector for each angular momentum channel.

In the case of the H atom, we have found that a high level of transferability was achieved without adding an augmentation operator, although addition of an augmentation operator did produce a slight improvement. For all other atoms we have found that a square potential step as the augmentation

TABLE V. Chemical hardness testing for the Ca atom. Absolute hardness values are compared for an all-electron atom (AE), a nonlocal pseudopotential generated with the method described in Ref. 4 (HSC), an optimized nonlocal pseudopotential generated with the method described in reference 14 (OPT) and a designed nonlocal pseudopotential generated with the presented method (DNL). Hardness values were determined for two different electronic configurations. Each element of the symmetric hardness matrix, $H_{nl,n'l'}$, is the change in the nlth eigenvalue (in Ry) for a change of the $n'l'$th occupation number.

		$3s^{1.95}3p^{5.9}4s^{1}3d^{0.1}$				$3s^{2}3p^{6}4s^{2}3d^{0.01}$			
nl	$n'l'$	AE	HSC	OPT	DNL	AE	HSC	OPT	DNL
$3s$	$3s$	0.5655	0.5670	0.5620	0.5657	0.4945	0.4946	0.4897	0.4946
	$3p$	0.5474	0.5453	0.5441	0.5475	0.4767	0.4735	0.4722	0.4767
	$4s$	0.2830	0.2853	0.2853	0.2830	0.2257	0.2269	0.2269	0.2257
	$3d$	0.4614	0.4612	0.4586	0.4614	0.3677	0.3654	0.3634	0.3677
$3p$	$3p$	0.5310	0.5250	0.5279	0.5309	0.4607	0.4540	0.4565	0.4606
	$4s$	0.2813	0.2832	0.2835	0.2813	0.2250	0.2260	0.2262	0.2250
	$3d$	0.4506	0.4491	0.4482	0.4507	0.3593	0.3562	0.3554	0.3594
$4s$	$4s$	0.2079	0.2095	0.2097	0.2079	0.1790	0.1799	0.1800	0.1790
	$3d$	0.2639	0.2654	0.2655	0.2639	0.2101	0.2105	0.2106	0.2101
$3d$	$3d$	0.3941	0.3928	0.3915	0.3936	0.2989	0.2959	0.2951	0.2986

operator gives improved transferability. The parameters for $\hat{A}$ are contained in Table II. Table III contains configurational testing results for the H, Si, and Ca atoms. Table IV contains testing results for Zr and Pb atoms. In both tables, the design configurations have been identified. For Ca and Zr atoms, for which semicore states were included, the reference configuration is also a design configuration due to the presence of the second s state. We present results from an all-electron atom, a nonlocal pseudopotential generated according to the Hamann-Schlüter-Chiang construction, an optimized pseudopotential generated with an unaugmented local potential consisting of only the s angular momentum channel potential, and a designed nonlocal pseudopotential which includes the square step. The potentials were tested in both ionized and excited electronic configurations. In addition to eigenvalue information, the table also compares total-energy differences from the reference state. It is important to note that the most substantial improvements occur in atoms in which highly spatially separated semicore states (Ca and Zr) were included in the pseudopotential construction. The inclusion of these states provides charge-density separation and therefore the placement of the augmentation operator in those regions of separation provides dramatic improvement [case (1) above]. The eigenvalue and total-energy errors for the Ca and Zr designed nonlocal pseudopotentials are one to two orders of magnitude smaller than the Hamann-Schlüter-Chiang and optimized results. For atoms in which charge separation is not as complete (Si and Pb), the improvements are less dramatic.

Logarithmic derivative determination has been extensively used as a testing procedure to investigate the transferability of a pseudopotential. For brevity we present only the results for the Ca pseudopotential. Figure 2 shows the logarithmic derivative differences between the all-electron potential and the three pseudopotential generation methods for the s, p, and d potentials of the Ca atom. For the s and p channels, we find excellent agreement over a large energy range between the pseudopotentials generated with the designed nonlocal method and the all-electron potentials. The energy errors in the s and p states for the Hamann-Schlüter-Chiang and optimized pseudopotentials presented in Table III are directly related to the logarithmic derivative differences. Interestingly, we find that the designed nonlocal pseudopotential d state logarithmic derivative differs from the all-electron results more than the other methods. This finding is in apparent contradiction to the configuration testing presented in Table III. The origin of the discrepancy lies in the nature of the logarithmic derivative test. This test only probes the behavior an electron of a given energy scattered off a static potential. Self-consistent effects are therefore not included. This phenomenon has been identified previously.[19] We find that chemical hardness testing tracks more closely with configuration testing than logarithmic derivative testing does. In logarithmic derivative testing at other electronic configurations, the designed nonlocal pseudopotential d state scattering properties are significantly more accurate than the other pseudopotentials.

Table V contains chemical hardness testing results for Ca all-electron and pseudoatoms, for two electronic configurations. In both cases, we find excellent agreement in chemical hardness between the all-electron and designed nonlocal potentials for each electronic configuration. With errors below 0.5 mRy, the designed nonlocal pseudopotential is one to two orders of magnitude more accurate than the Hamann-Schlüter-Chiang and optimized pseudopotentials. All matrix elements involving the $3d$ state show a higher level of transferability for the designed nonlocal pseudopotential than the other pseudopotentials.

TABLE VI. Density-functional results for various diatomic and bulk systems. Structural parameters are compared for a nonlocal pseudopotential generated with the method described in Ref. 4 (HSC), an optimized nonlocal pseudopotential generated with the method described in Ref. 14 (OPT) and a designed nonlocal pseudopotential generated with the presented method (DNL). Experimental and previous theoretical results using dual-space (DS) pseudopotentials and linearized-augmented plane-wave (LAPW) methods are also provided for comparison.

	Expt.	DS	LAPW	HSC	OPT	DNL
			H_2			
r_e (Å)	0.741 [a]	0.766 [b]	0.773 [c]	0.767	0.766	0.767
ω_e (cm^{-1})	4395		4040	4169	4178	4165
			Si(s)			
a (Å)	5.43 [d]		5.41 [e]	5.363	5.361	5.412
B (GPa)	98.8		98	96.2	98.1	96.0
			SiH_4			
r_e (Å)	1.479 [f]	1.486		1.485	1.482	1.491
ν_1 (cm^{-1})	2187			2140	2145	2182
			Ca(s)			
a (Å)	5.58 [d]		5.33 [e]	5.332	5.332	5.338
B (GPa)	15.2		19	19.1	19.2	19.4
			CaH			
r_e (Å)	2.002 [a]	1.961		1.954	1.950	1.954
ω_e (cm^{-1})	1299			1290	1275	1285
			Zr(s)			
a (Å)	3.232 [d]		3.145 [g]	3.122	3.120	3.161
c (Å)	5.147		5.116	5.047	5.043	5.122
B (GPa)	83.3		98.6	102.9	105.0	93.4
			Pb(s)			
a (Å)	4.95 [d]			4.866	4.859	4.868
B (GPa)	43.0			55.0	55.2	55.0
			PbH			
r_e (Å)	1.839 [a]	1.817		1.852	1.850	1.853
ω_e (cm^{-1})	1564			1536	1579	1530

[a]Reference 20.
[b]Reference 16.
[c]Reference 23.
[d]Reference 21.
[e]Reference 24.
[f]Reference 22.
[g]Reference 25 using Hedin-Lundqvist exchange-correlation potentials.

As a final set of tests, we have completed density-functional calculations within the LDA for various hydride molecules involving the presented atoms as well as bulk Si, Ca, Zr, and Pb. The results of these tests are contained in Table VI. We also provide experimental results[20–22] and theoretical studies where available.[16,23–25] The cited linearized-augmented plane-wave (LAPW) calculations[23–25] treat all

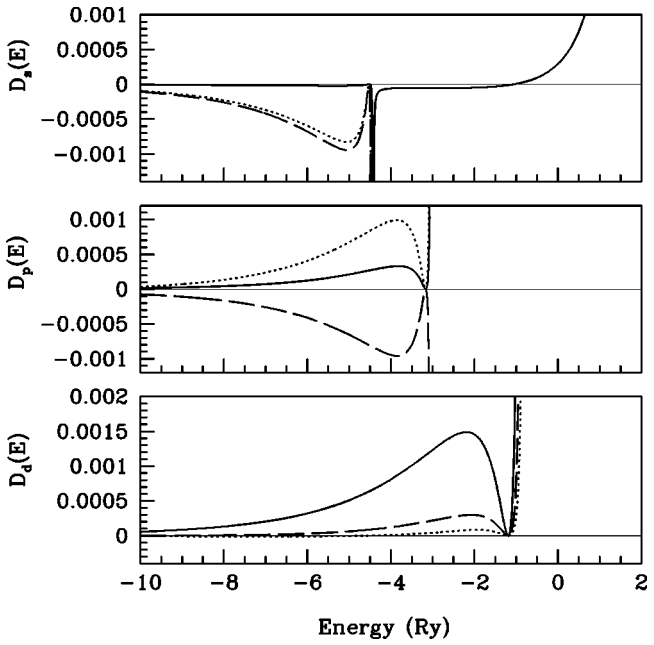

FIG. 2. Differences in logarithmic derivatives between the Ca pseudopotential and the all-electron calculation for the s (top), p (middle), and d (bottom) states at the reference configuration ($3s^2 3p^6 4s^0 3d^0$). Results are given for a nonlocal pseudopotential (dotted line) generated with the method described in Ref. 4, an optimized nonlocal pseudopotential (dashed line) generated with the method described in Ref. 14, and a designed nonlocal pseudopotential generated with the presented method (solid line).

the electrons explicitly. The dual-space pseudopotential calculations[16] treat the valence electrons explicitly; for Ca, a shell of semicore states is also included. Typically, structural parameters computed using LDA underestimate the experimental values by 1–2 %. For the hydride calculations, results differ from the expected underestimation due to the core overlap with the H pseudopotential. All the pseudopotentials show very similar results for the H_2, SiH_4, and CaH. In the case of PbH, our deviation from the previous theoretical results using highly transferable dual-space pseudopotentials can be explained by the omission of the $5d$ semicore state in the dual-space construction. For the bulk materials, we find good agreement with the LAPW method results which represent the LDA computational limit of these structural properties. In the case of bulk Zr, we find that the use of the designed nonlocal potential has a significant effect on the calculation of structural parameters. This improvement is due to the considerable transferability enhancement which the designed nonlocal approach provides (see Table IV). Since Zr is a transition metal, its s and d orbitals are very similar in energy; this makes the structural parameters of Zr more sensitive to the pseudopotential transferability than the other elements tested.

It is important to note that the calculation of these structural parameters is very robust and is therefore not a particularly sensitive test of transferability. Instead, studies involving electronic properties of systems such as electron-phonon interactions may be more fruitful in ascertaining the effects of improved transferability.

IV. CONCLUSIONS

In this paper, we have developed and implemented a fully nonlocal pseudopotential approach using the separable form of Kleinman and Bylander. In our approach, we have exploited the implicit flexibility contained within the separation of the pseudopotential into local and nonlocal parts by including an augmentation operator into the local and nonlocal parts of the potential. By adjusting the augmentation operator, we have been able to achieve almost exact agreement with all-electron results for a variety of ionized and excited configurations. In addition to configuration testing, we have presented logarithmic derivatives and chemical hardness tests. All the tests demonstrate significant improvement of the designed pseudopotentials over Hamann-Schlüter-Chiang and standard nonlocal potentials. The designed nonlocal pseudopotential approach is able to achieve these improvements in transferability without compromising the level of convergence error obtained using the optimized pseudopotential construction. Furthermore, we have shown that for electronic configurations that contain multiple states with the same angular momentum, it is possible to construct a pseudopotential with a single nonlocal projector that will yield very accurate results.

ACKNOWLEDGMENTS

The authors are thankful for helpful discussions with S. P. Lewis during the preparation of this manuscript. This work was supported by the Laboratory for Research on the Structure of Matter and the Research Foundation at the University of Pennsylvania as well as NSF Grant No. DMR 97-02514 and the Petroleum Research Fund of the American Chemical Society (Grant No. 32007-G5). Computational support was provided by the San Diego Supercomputer Center and the National Center for Supercomputing Applications.

[1] J. C. Phillips and L. Kleinman, Phys. Rev. **116**, 287 (1959).
[2] C. Herring, Phys. Rev. **57**, 1169 (1940).
[3] For example, see T. Starkloff and J. D. Joannopoulos, Phys. Rev. B **16**, 3562 (1977).
[4] D. R. Hamann, M Schlüter, and C. Chiang, Phys. Rev. Lett. **43**, 1494 (1979).
[5] L. Kleinman and D. M. Bylander, Phys. Rev. Lett. **48**, 1425 (1982).
[6] X. Gonze, P. Käckell, and M. Scheffler, Phys. Rev. B **41**, 12 264 (1990).
[7] X. Gonze, R. Stumpf, and M. Scheffler, Phys. Rev. B **44**, 8503 (1991).
[8] R. D. King-Smith, M. C. Payne, and J. S. Lin, Phys. Rev. B **44**, 13 063 (1991).
[9] S. Goedecker, Philos. Mag. **70**, 305 (1994); C. Y. Wei, S. P. Lewis, E. J. Mele, and A. M. Rappe, Phys. Rev. B **55**, 15 356

(1997); S. P. Lewis, C. Y. Wei, E. J. Mele, and A. M. Rappe, Phys. Rev. B **58**, 3482 (1998).
[10] D. C. Allan and M. P. Teter, Phys. Rev. Lett. **59**, 1136 (1987).
[11] P. E. Blöchl, Phys. Rev. B **41**, 5414 (1990).
[12] D. Vanderbilt, Phys. Rev. B **41**, 7892 (1990).
[13] M. Teter, Phys. Rev. B **48**, 5031 (1993).
[14] A. M. Rappe, K. M. Rabe, E. Kaxiras, and J. D. Joannopoulos, Phys. Rev. B **41**, 1227 (1990).
[15] A. Filippetti, A. Satta, D. Vanderbilt, and W. Zhong, Int. J. Quantum Chem. **61**, 421 (1997).
[16] C. Hartwigsen, S. Goedecker, and J. Hutter, Phys. Rev. B **58**, 3641 (1998).
[17] S. Goedecker, M. Teter, and J. Hutter, Phys. Rev. B **54**, 1703 (1996).
[18] D. D. Koelling and B. N. Harmon, J. Phys. C **10**, 3107 (1977).
[19] S. Goedecker and K. Maschke, Phys. Rev. A **45**, 88 (1992).
[20] G. Herzberg, *Molecular Spectroscopy and Molecular Structure* (Van Nostrand Reinhold, New York, 1950), Vol. 1, and references therein.
[21] C. Kittel, *Introduction to Solid State Physics*, 7th ed. (Wiley, New York, 1996), and references therein.
[22] G. Herzberg, *Molecular Spectroscopy and Molecular Structure* (Van Nostrand Reinhold, New York, 1950), Vol. 3, and references therein.
[23] P. E. Blöchl, Phys. Rev. B **50**, 17 953 (1994).
[24] N. A. W. Holzwarth, G. E. Matthews, R. B. Dunning, A. R. Tackett, and Y. Zeng, Phys. Rev. B **55**, 2005 (1997).
[25] Z.-W. Lu, D. Singh, and H. Krakauer, Phys. Rev. B **36**, 7335 (1987).